

Updraft Model for Development of Autonomous Soaring Uninhabited Air Vehicles

Michael J. Allen*

NASA Dryden Flight Research Center, Edwards, California 93523-0273, USA

Large birds and glider pilots commonly use updrafts caused by convection in the lower atmosphere to extend flight duration, increase cross-country speed, improve range, or simply to conserve energy. Uninhabited air vehicles may also have the ability to exploit updrafts to improve performance. An updraft model was developed at NASA Dryden Flight Research Center (Edwards, California) to investigate the use of convective lift for uninhabited air vehicles in desert regions. Balloon and surface measurements obtained at the National Oceanic and Atmospheric Administration Surface Radiation station (Desert Rock, Nevada) enabled the model development. The data were used to create a statistical representation of the convective velocity scale, w^* , and the convective mixing-layer thickness, z_i . These parameters were then used to determine updraft size, vertical velocity profile, spacing, and maximum height. This paper gives a complete description of the updraft model and its derivation. Computer code for running the model is also given in conjunction with a check case for model verification.

Nomenclature

C_p	= specific heat of dry air, J/kg ^o K
e_s	= saturated vapor pressure, mb
e_v	= vapor pressure, mb
g	= gravitational constant, m/s ²
h	= height above ground, m
j	= ground measurement sample index
k_i	= shape constant, unitless
L	= straight line length, m
max	= maximum
n	= ground measurement sample index at sunset
N	= number of updrafts inside a given area
N_L	= number of updrafts encountered along straight line
p	= surface pressure, mb
p_0	= reference pressure, mb
PDF	= probability density function
Q_G	= heat into ground, W/m ²
\tilde{Q}_H	= sensible heat flux, W/m ²
Q_H	= kinematic sensible heat flux, °K*m/s
Q_{OV}	= surface virtual potential temperature flux, W/m ²
Q_S	= net radiation at surface, W/m ²
r	= distance to updraft center, m
r_1	= updraft core radius, m
r_2	= updraft outer radius, m
rh	= relative humidity, percent
SURFRAD	= Surface Radiation
s_{wd}	= downdraft velocity ratio, unitless
T	= temperature, °C

* Aerospace Engineer, Controls and Dynamics Branch, P.O. Box 273/MS-4840D, Member.

T_s	= surface temperature, °C
UAV	= uninhabited air vehicle
w	= updraft velocity, m/s
w^*	= convective velocity scale, m/s
w_I	= intermediate variable in downdraft velocity calculation, m/s
w_c	= updraft velocity corrected for environment sink, m/s
w_D	= downdraft velocity, m/s
w_e	= environment sink velocity, m/s
w_{peak}	= maximum vertical velocity, m/s
w_s	= mixing ratio, g/kg
\bar{w}	= average updraft velocity, m/s
X	= test area length, m
Y	= test area width, m
z	= aircraft height, m
z_i	= convective mixing-layer thickness, m

β	= Bowen ratio, unitless
ρ	= moist air density, kg/m ³
θ_0	= surface potential temperature, °K
σ	= standard deviation
Γ_D	= dry adiabatic lapse rate, °C/m
ψ	= angular position, rad
$\bar{\theta}_0$	= daily average surface potential temperature, °K

I. Introduction

One relatively unexplored way to improve the range, duration, or cross-country speed of an autonomous aircraft is to use buoyant plumes of air found in the lower atmosphere, known as *thermals* or *updrafts*. Updrafts occur when the air near the ground becomes less dense than the surrounding air because of heating or humidity changes at the surface of the Earth. Piloted sailplanes rely solely on this free energy to make flights of more than 2000 kilometers.¹ Soaring birds such as hawks and vultures have been observed to circle for hours without flapping their wings; and Frigatebirds are known to soar continuously, day and night, using updrafts.²

Many uninhabited air vehicles (UAVs) have similar sizes, wing loadings, and missions as soaring birds and sailplanes. Such missions that could allow small UAVs to take advantage of updrafts encompass remote sensing, surveillance, atmospheric research, communications, and Earth science. A previous study using a simple UAV simulation with updrafts calculated from measured surface and balloon data found that a 2-hr nominal-endurance UAV can potentially gain 12 hr of flight time during the summer and 5 hr of flight time during the winter using updrafts.³

Researchers have used various updraft models to study optimal soaring paths,⁴ glider design,⁵ and cloud formation.⁶ Wharington used a simple updraft model to develop algorithms for a soaring UAV.⁷ These models generally provide a vertical velocity distribution for a given radius and peak updraft velocity. This paper presents a unique updraft model in that statistical values for updraft velocity, convective mixing-layer thickness, updraft spacing, and updraft size are determined from measured data.

II. Convective-Layer Scale Factors

The convective velocity scale, w^* , and convective mixing-layer thickness, z_i , were calculated from surface and rawinsonde balloon measurements taken at the National Oceanic and Atmospheric Administration (NOAA) Surface Radiation (SURFRAD) station in Desert Rock, Nevada (lat. 36.63 deg N, long. 116.02 deg W, elev. 1007 m). The convective layer is the lowest region of the atmosphere where significant mixing occurs. During calm conditions, buoyant plumes of air that have been heated at the surface cause local mixing. These plumes of air, called *updrafts* or *thermals*, can have significant upward velocity.

SURFRAD instrumentation includes a radiometer platform, meteorology tower, and solar tracker. Measurements were taken every 3 min. A rawinsonde station is also collocated with the SURFRAD site where rawinsonde balloons

were launched every 12 hr. This study used surface temperature, wind, and radiation measurements as well as balloon-measured temperature and humidity collected from the entire year of 2002.⁸

The convective mixing-layer thickness, z_i , as Fig. 1 shows, is the maximum height-above-ground that updrafts generally obtain. The mixing-layer thickness was calculated using predawn rawinsonde balloon data and measured surface temperatures. The convective mixing-layer thickness was estimated by finding the intersection of the predawn balloon-measured temperature profile as a function of altitude with the line given by Eq. (1).

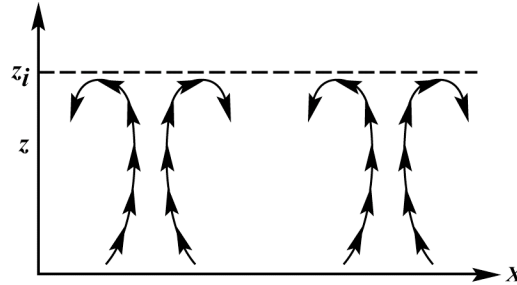


Figure 1. Simplified representation of atmosphere with updrafts showing convective mixing-layer thickness, z_i .

$$T = -\Gamma_D h + T_s \quad (1)$$

The line defined by Eq. (1) gives a temperature, T , for every height, z , using the dry adiabatic lapse rate, Γ_D , of $0.00975 \text{ }^\circ\text{C/m}$. Figure 2 shows an example of the z_i calculation.

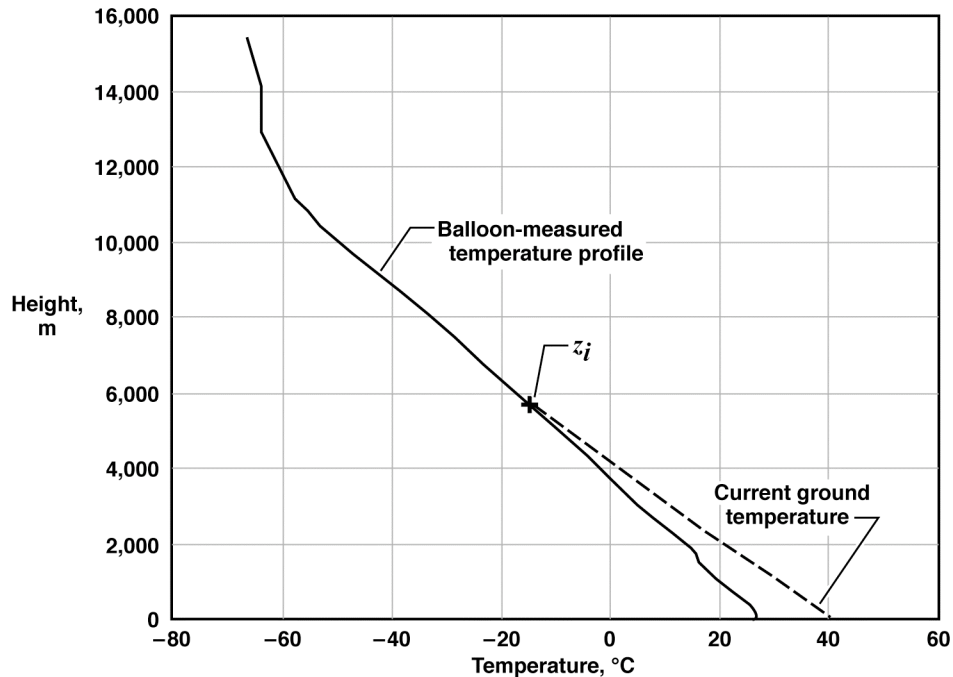


Figure 2. Example of z_i calculation.

A surface heat budget was used to calculate the convective velocity scale, w^* . The first step in this process is to calculate the sensible heat flux, \tilde{Q}_H , given by Stull in Eq. (2).⁹

$$\tilde{Q}_H = \frac{\beta(-Q_S + Q_G)}{(1+\beta)} \quad (2)$$

In this equation, \tilde{Q}_H is the sensible heat flux, Q_S is the net radiation at the surface, Q_G is the heat into the ground, and β is the Bowen ratio, defined as the ratio of sensible to latent heat fluxes at the surface. This study uses a Bowen ratio of 5, given for semi-arid regions.⁹ The net radiation, Q_S , was measured directly by the SURFRAD station; and the heat into the ground, Q_G , was calculated applying Eq. (3) taken from Stull⁹ using the percentage method for daytime calculations.

$$Q_G = 0.1Q_S \quad (3)$$

Sensible heat flux was then converted to its kinematic form using Eq. (4).

$$Q_H = \frac{\tilde{Q}_H}{\rho C_p} \quad (4)$$

Values for the density of moist air, ρ , and the specific heat of dry air, C_p , used in Eq. (4), were 1.210 kg/m³ and 1004.67 J/kg^oK, respectively. The surface virtual potential temperature flux, Q_{OV} , was then calculated with Eq. (5) using the definition of virtual potential temperature for unsaturated air.⁹

$$Q_{OV} = Q_H(1 + 0.61w_s) \quad (5)$$

Equation (5) was solved using the mixing ratio, w_s , calculated from Eq. (6).

$$w_s = \frac{622ev}{p - ev} \quad (6)$$

In Eq. (6), p is the surface pressure and ev is the vapor pressure given by Eq. (7).

$$ev = rh \cdot es/100 \quad (7)$$

Equation (7) was solved using the measured relative humidity, rh , and saturated vapor pressure, es , calculated from Eq. (8).

$$es = 6.112e^{\frac{17.67T_s}{T_s + 243.5}} \quad (8)$$

Equation (8) was solved using measured surface temperature, T_s . Equations (2) to (8) determine the surface heat budget required to calculate Q_{OV} . Equation (9) calculates the convective scaling velocity.

$$w^* = \left(Q_{OV} z_i \frac{g}{\bar{\theta}_0} \right)^{\frac{1}{3}} \quad (9)$$

In Eq. (9), g is the gravitational constant and $\bar{\theta}_0$ is the daily average surface potential temperature given by Eq. (10).

$$\bar{\theta}_0 = \frac{\sum_{j=1}^n \left(T_{s_j} + 273.15 \right) \left(\frac{p_0}{p_j} \right)^{0.286}}{n} \quad (10)$$

Equation (10) was solved using measured surface temperature, T_s , and pressure, p , and a reference pressure, p_0 , of 1000 mb. The sample index, $j = 1$, refers to sunrise and $j = n$ refers to sunset. The convective velocity scale, w^* , is used primarily to calculate the updraft vertical velocity. The convective scale velocity was set to zero if the surface wind velocity was greater than 12.87 m/s (25 knots) to account for the disruptive effect of high winds on updrafts.

III. Test Point Matrix

This study uses statistical tools to summarize yearly and daily changes in z_i and w^* into a set of representative cases. The histogram in Fig. 3 shows the distribution of w^* for all daylight hours during the year 2002. Data points that produced a convective velocity scale of zero comprise 25 percent of the total set of recorded data and were not included in the Fig. 3 histogram. Zero convective mixing-layer thickness, zero net radiation, or high winds can cause zero scale velocity. Of these causes, the most prevalent was found to be zero net radiation because of low sun angles during early morning and late evening.

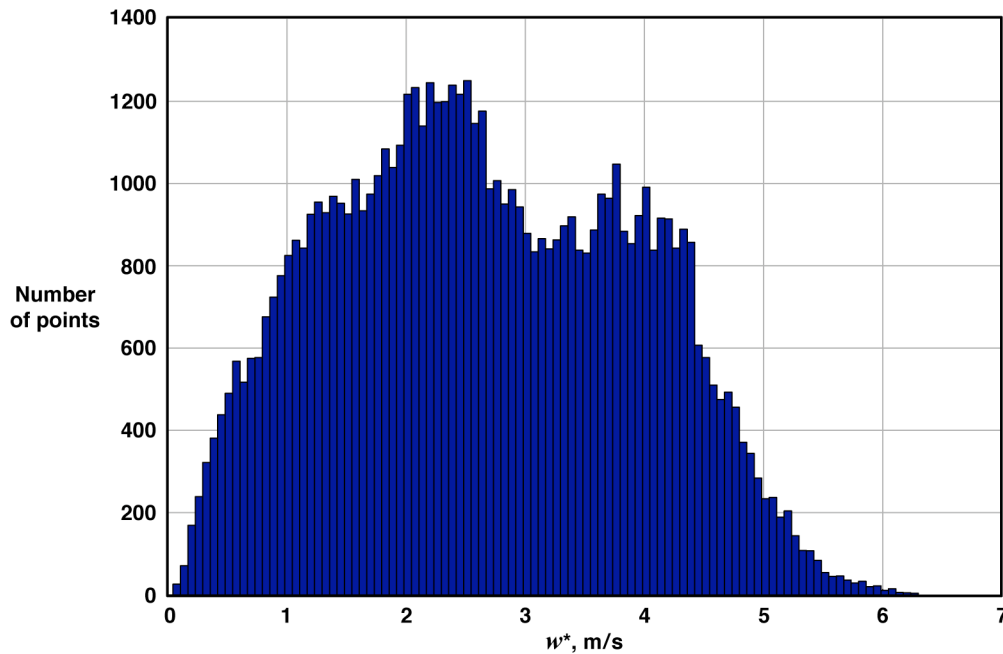


Figure 3. The w^* histogram for all samples during daylight hours of 2002, when updrafts were present.

A statistical representation of w^* was found using percentiles. The following percentiles were chosen as test points: 2.3, 15.9, 50.0, 84.1, and 97.7. The five test cases are referred to as -2σ , -1σ , mean, $+1\sigma$, and $+2\sigma$ because they are analogous to the standard deviation and mean values of a Gaussian probability density function (PDF). The use of percentiles allowed the calculation of a simple set of test cases to represent the distribution of convective velocity scale.

A distribution of all z_i values for each selected w^* in the test point matrix was created by collecting all z_i points corresponding to w^* values that fell within a window of ± 0.1 m/s from the selected test point w^* . Figure 4 shows an example of the z_i data selection for a given w^* . A Gamma PDF was used to model the statistics of z_i . The Gamma PDF coefficients that best fit the data were used to calculate the -1σ , mean, and $+1\sigma$ points in the test point matrix. Table 1 gives the resulting set of convective scale factor test points.

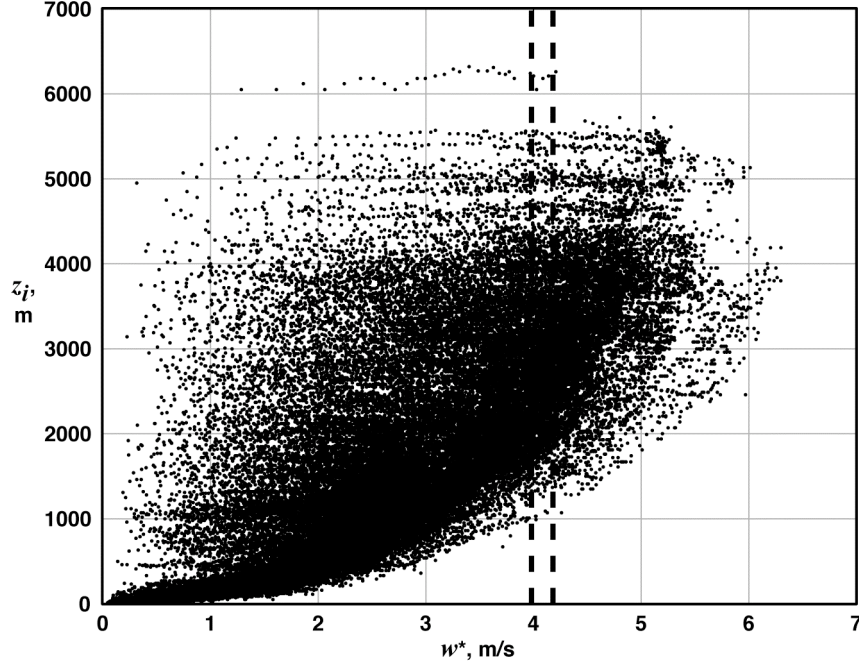


Figure 4. Convective mixing-layer thickness, z_i , as function of convective velocity scale, w^* . (Dashed lines indicate z_i window for the example case of $w^* = 4.08$ m/s.)

Table 1. Convective scale test points during times when updrafts are present.

Description	w^* , m/s	$-1\sigma z_i$, m	mean z_i , m	$+1\sigma z_i$, m
$-2\sigma w^*$	0.46	25.6	53.6	97.4
$-1\sigma w^*$	1.27	150	210	1007
mean w^*	2.56	767	1401	2319
$+1\sigma w^*$	4.08	2134	2819	3638
$+2\sigma w^*$	5.02	2913	3647	4495

The test conditions given in Table 1 indicate the year-round statistical properties of convective lift during times when updrafts were present. These test points include variations in convection as a result of time of day and time of year. Table 1 shows large variations of w^* and z_i , illustrating the challenge presented to a soaring aircraft that must use as many updraft sizes and strengths as possible.

Table 2 presents monthly trends. These points represent the mean and maximum values of w^* during the daylight hours of the selected month. The z_i test points in Table 2 were found by taking the mean of all z_i points in the selected month that fell within a window of ± 0.1 m/s from the selected test point w^* . Test points given in Table 2 reveal the seasonal variations in updraft strength and altitude. Daily variations are generally sinusoidal, with zero w^* at sunrise, maximum w^* near noon, and zero w^* at sunset.

Table 2. Monthly convective scale test points for all times between sunrise and sunset.

	Jan	Feb	Mar	Apr	May	Jun	Jul	Aug	Sep	Oct	Nov	Dec
mean w^* , m/s	1.14	1.48	1.64	1.97	2.53	2.38	2.69	2.44	2.25	1.79	1.31	1.26
z_i for mean w^* , m	504	666	851	1213	1887	1728	1975	1755	1382	893	627	441
max w^* , m/s	3.59	3.97	4.89	5.53	5.49	5.51	6.30	5.64	5.97	4.57	4.55	4.11
z_i for max w^* , m	1800	1970	3900	2380	3833	4027	3962	4940	2460	3285	1783	1680

IV. Updraft Calculations

Each w^* and z_i scaling parameter given in Table 1 and Table 2 can be used to calculate updraft velocity, radius, and vertical velocity distribution using the equations provided in this section. Equation (11) taken from Lenschow¹⁰ calculates average updraft velocity using height, z , and the convective-layer scale parameters, w^* and z_i , from Table 1 or Table 2.

$$\bar{w} = w^* \left(\frac{z}{z_i} \right)^{\frac{1}{3}} \left(1 - 1.1 \frac{z}{z_i} \right) \quad (11)$$

Figure 5 is a plot of Eq. (11). The maximum vertical velocity of $0.45 w^*$ occurs at a height ratio, z/z_i , of approximately 0.25. Also note that the updraft velocity is negative for height ratios greater than 0.9. The height at which peak vertical velocity occurs is lower than those published by Bradbury.¹¹ The dissimilarities may occur because of differing climate, topography, or definition of the convective mixing-layer thickness.

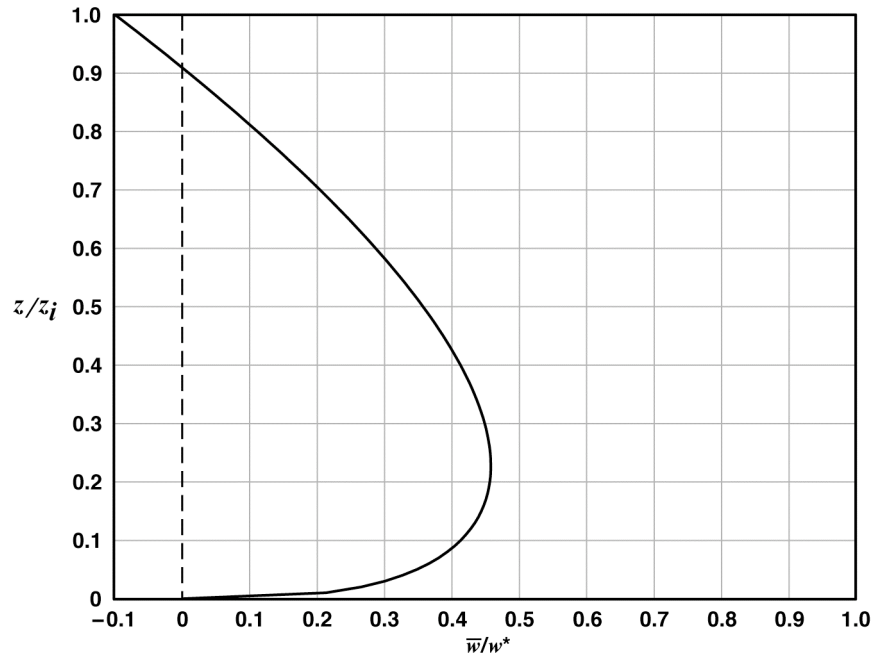


Figure 5. Updraft mean vertical velocity ratio as function of height ratio.

Equation (12) calculates updraft outer radius, r_2 , as determined by Lenschow.¹⁰

$$r_2 = \max \left(10, 0.102 \left(\frac{z}{z_i} \right)^{\frac{1}{3}} \left(1 - 0.25 \frac{z}{z_i} \right) * z_i \right) \quad (12)$$

Equation (12) predicts small updraft outer radius near the ground and an increasingly larger updraft radius as height increases. Figure 6 shows updraft outer radius ratio, r_2/z_i . Updraft radius is independent of velocity in this model.

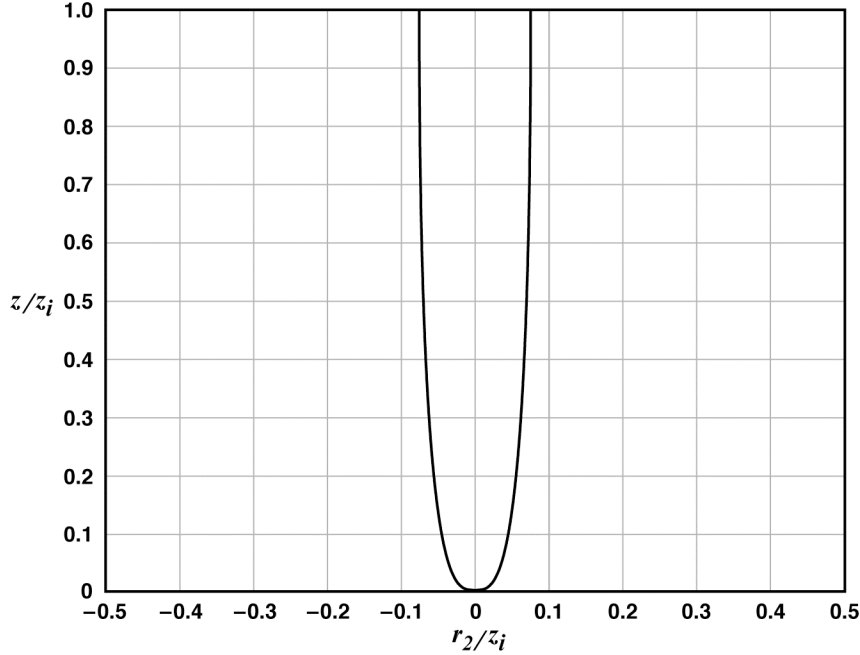


Figure 6. Ratio of outer radius to convective mixing-layer thickness, r_2/z_i , as function of height ratio, z/z_i .

The distribution of vertical velocity within the updraft varies considerably between updrafts. The literature contains various updraft vertical velocity distributions. Wharington^{7, 12} used Gaussian-shaped updrafts to study autonomous soaring techniques and Metzger and Hedrick⁴ used simple square-edged lift regions to optimize flight paths for cross-country flight. Many references depict updrafts to be quite random in size and updraft velocity distribution. In the book *Cross Country Soaring*,¹³ Helmut Reichmann states that thermals are “seldom, if ever, round” and “the thermals that depart from the norm are most likely the norm itself.”

Flight test results were used in an attempt to model the distribution of vertical velocity for the updraft model presented in this paper. Flight tests conducted by Konovalov¹⁴ show two basic vertical velocity profiles, called *type-a* and *type-b*. Type-a updrafts are strong and have a wide area of nearly constant lift. Type-b updrafts are weaker and have increasingly more lift toward the center. Konovalov also correlated the frequency of occurrence of type-a and type-b updrafts to the updraft diameter. This paper uses Konovalov’s data to correlate the vertical velocity distribution of an updraft to its outer radius. Figure 7 shows a revolved trapezoid that was used to fit Konovalov’s type-a and type-b updrafts by adjusting the inner radius, r_1 . This study uses a revolved trapezoid because the trapezoid provided a good approximation to the vertical velocity profiles given by Konovalov. A fit of Konovalov’s data yields the piecewise function for the updraft radius ratio, r_1/r_2 , given in Eq. (13).

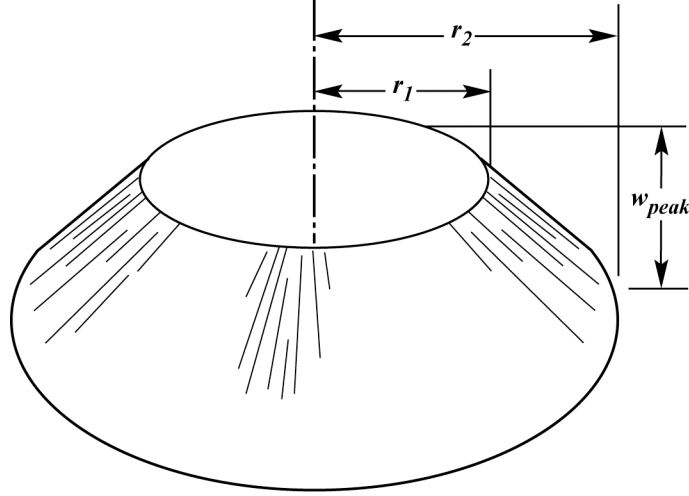


Figure 7. Revolved trapezoid vertical velocity distribution.

$$\frac{r_1}{r_2} = \begin{cases} 0.0011 * r_2 + 0.14 & \text{for } r_2 < 600\text{m} \\ 0.8 & \text{else} \end{cases} \quad (13)$$

The average vertical velocity of a revolved trapezoid updraft distribution is found by dividing the volume of the revolved trapezoid shape by the base area. Equation (14) gives the resulting relationship.

$$\bar{w} = \frac{1}{\pi r_2^2} \int_0^{2\pi} \left[\int_0^{r_1} w_{peak} * r * dr + \int_{r_1}^{r_2} \frac{w_{peak} (r_2 - r)}{r_2 - r_1} r * dr \right] d\psi \quad (14)$$

Evaluating Eq. (14) and solving for w_{peak} gives the relationship found in Eq. (15).

$$w_{peak} = \frac{3\bar{w}(r_2^3 - r_2^2 r_1)}{r_2^3 - r_1^3} \quad (15)$$

Equation (15) determines the peak value, w_{peak} , of a revolved trapezoid updraft distribution for a given average updraft velocity, w_T . The vertical velocity distribution was further refined by fitting a bell shape given in Eq. (16) to approximate the revolved trapezoid distribution. A bell shape was chosen because the bell shape defines a smooth vertical velocity distribution.

$$w = w_{peak} \left(\frac{1}{1 + \left| k_1 * \frac{r}{r_2} + k_3 \right|^{k_2}} + k_4 * \frac{r}{r_2} + w_D \right) \quad (16)$$

In Eq. (16), k_{1-4} are shape constants and w_D is the downdraft velocity. This equation describes a family of curves designed to fit the trapezoid shape given by Eq. (13) for a range of discrete r_1/r_2 values. Seven evenly spaced points

were chosen to represent the range of possible vertical velocity distributions. Table 3 gives the shape constants used in Eq. (16) for each r_1/r_2 ratio. Figure 8 shows the resulting family of updraft velocity distributions. The downdraft velocity term, w_D , simulates the toroid-like downward velocity found on the outer edge of updrafts as described by Bradbury. Figure 9 illustrates the toroid shape of the updraft as the updraft increases in height. Eqs. (17) and (18) calculate the downdraft velocity.

Table 3. Shape constants for bell-shaped vertical velocity distribution.

r_1/r_2	k_1	k_2	k_3	k_4
0.14	1.5352	2.5826	-0.0113	0.0008
0.25	1.5265	3.6054	-0.0176	0.0005
0.36	1.4866	4.8354	-0.0320	0.0001
0.47	1.2042	7.7904	0.0848	0.0001
0.58	0.8816	13.972	0.3404	0.0001
0.69	0.7067	23.994	0.5689	0.0002
0.80	0.6189	42.797	0.7157	0.0001

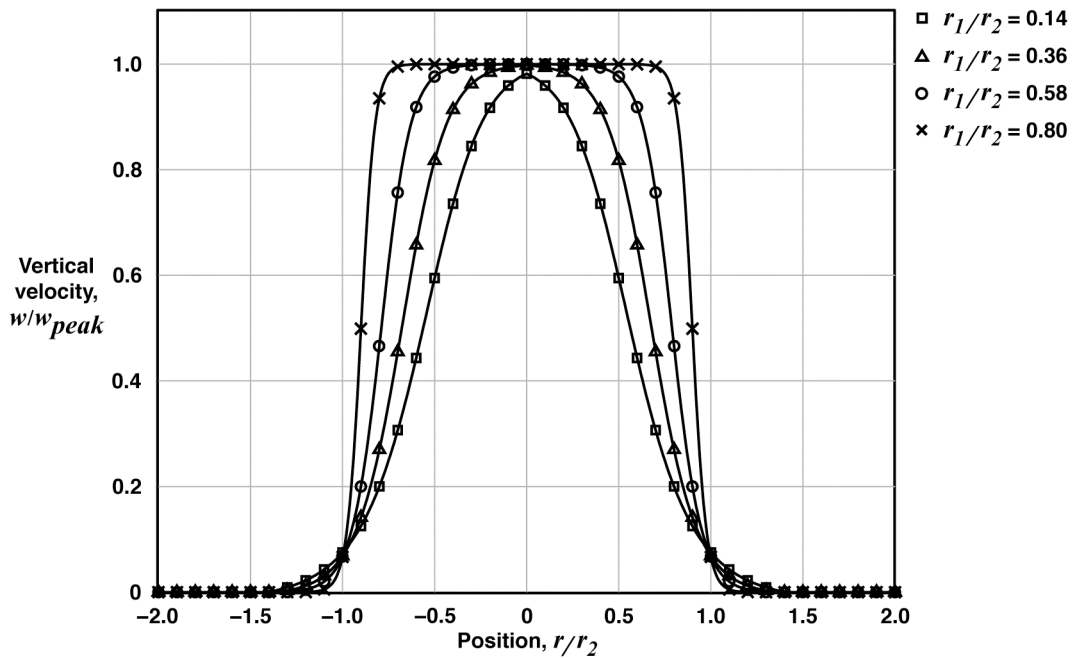


Figure 8. Bell-shaped vertical velocity distributions.

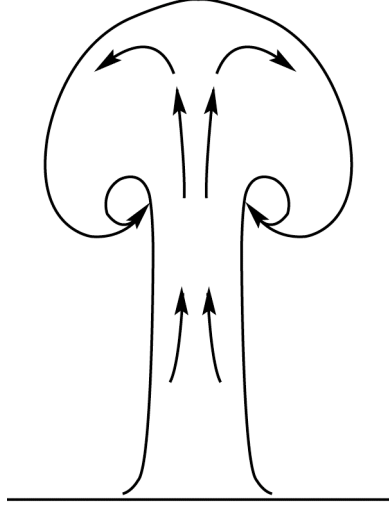


Figure 9. Development of updraft toroid shape as height increases.

$$w_I = \begin{cases} \frac{-\pi}{6} \sin\left(\frac{\pi * r}{r_2}\right) & \text{for } r_1 < r < 2r_2 \\ 0 & \text{else} \end{cases} \quad (17)$$

$$w_D = \begin{cases} 2.5w_I \left(\frac{z}{z_i} - 0.5\right) & \text{for } 0.5 < \frac{z}{z_i} < 0.9 \\ 0 & \text{else} \end{cases} \quad (18)$$

Additionally, Eqs. (17) and (18) modify the vertical velocity shape given in Eq. (16) to have zero net vertical velocity when $z/z_i = 0.9$. The height ratio 0.9 was chosen because the vertical velocity of the updraft is negative at altitudes above 0.9 as given in Eq. (11). Figure 10 gives vertical velocity profiles for low and high updrafts. The vertical velocity profiles show increasing downdraft at the outer edge of the updraft as height is increased. Figure 10 was generated with the convective velocity scale, w^* , and convective mixing-layer thickness, z_i , of 2.56 m/s and 1401 m, respectively.

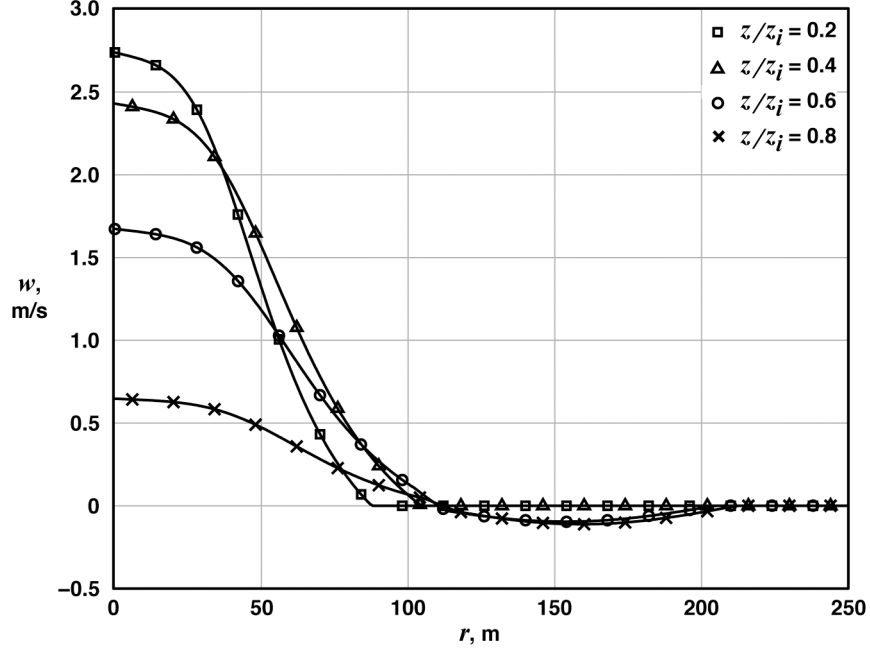


Figure 10. Vertical velocity profiles of a typical updraft with increasing height.

V. Updraft Spacing and Environment Sink

Updraft spacing was determined from Lenschow¹⁰ for a constant z/z_i of 0.4. Equation (19) gives the resulting relationship.

$$\frac{N_L z_i}{L} = 1.2 \quad (19)$$

In Eq. (19), N_L is the number of updrafts encountered along a straight line of length, L . Equation (20) solves for the number of updrafts within a given area of length, X , and width, Y , and a given updraft outer radius, r_2 .

$$N = \frac{0.6YX}{z_i r_2} \quad (20)$$

In a given test area, all upward moving air in the form of updrafts is balanced by an equal amount of downward moving air, known as *environment sink*, in the surrounding atmosphere. Environment sink is applied whenever the aircraft is not inside an updraft. Conservation of mass was used to determine the environment sink velocity for a given test area. Equation (21) gives the resulting relationship.

$$w_e = \frac{-\bar{w} N \pi r_2^2 s_{wd}}{X * Y - N \pi r_2^2} \quad (21)$$

Equation (21) relates the environment sink velocity, w_e , to the average updraft velocity, \bar{w}_T , using the downdraft velocity ratio, s_{wd} , given in Eq. (22).

$$s_{wd} = \frac{w_D}{w_I} \quad (22)$$

The downdraft velocity ratio is used to modify the environment sink calculation to account for the downward moving air defined in Eqs. (17) and (18). The vertical velocity distribution of the updraft can be blended to match the environment sink at the outer radius of the updraft using Eq. (23).

$$w_c = w \left(1 - \frac{w_e}{w_{peak}} \right) + w_e \quad (23)$$

Equation (23) stretches the vertical velocity distribution to maintain the maximum vertical velocity at the center of the updraft while allowing a smooth transition to the environment sink at the outer edge of the updraft.

VI. Application

This paper presents an updraft model for a specific intention—to use the model during the design and simulation of autonomous soaring UAVs. This section introduces an example set of updraft calculations for a typical simulation case. Appendix A gives a MATLAB® (The MathWorks, Natick, Massachusetts) script for this example. The convective scale factors, w^* and z_i , were taken from the mean values given in Table 1 to be 2.56 m/s and 1401 m, respectively, for this example. The height, z , used in this example was chosen as 280 m, giving a height ratio, z/z_i , of 0.2. Calculating the updraft outer radius, r_2 , from Eq. (12) yielded 79.4 m. The number of updrafts in the test area (defined by $X=1000$ m and $Y=1000$ m) calculated from Eq. (20) was five, using $r_2 = 79.4$ m and $z_i = 1401$ m. The resulting five updrafts can be positioned anywhere within the test area. Updrafts were positioned evenly along a diagonal line in this example for clarity. The vertical velocity of the test area was calculated with Eqs. (11) to (18) and (21) to (23) of this paper for every point within the test area using a grid spacing of 10 m. Figure 11 shows the resulting vertical velocities of the test area. Figure 12 shows the vertical velocity distribution of a single updraft as a check case for the code given in Appendices A and B. Figure 12 of this paper was produced with the MATLAB script given in Appendix A. Electronic copies of this code can be obtained from the author.

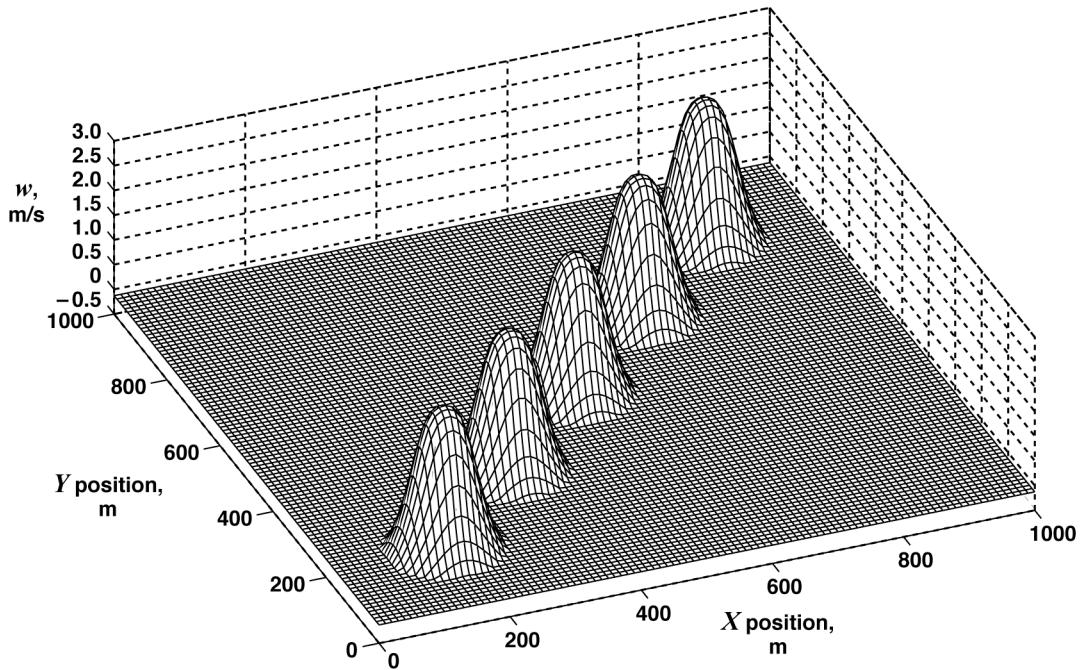


Figure 11. Example test area (calculated from MATLAB code given in Appendix A). Updrafts are positioned along a line for clarity.

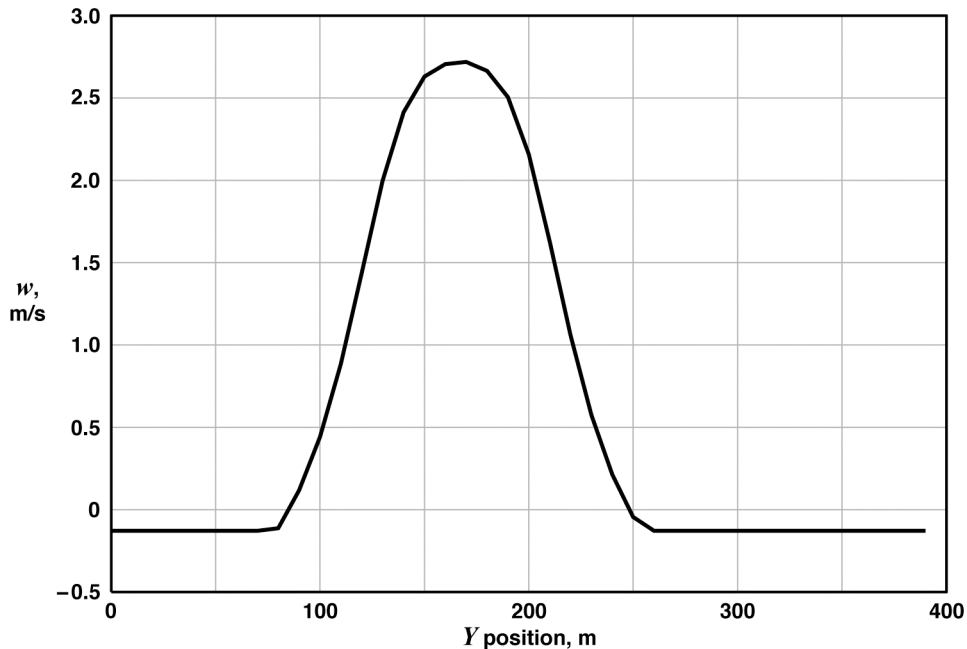


Figure 12. Vertical velocity profile check case (calculated from MATLAB code given in Appendix A).

The updraft positions should be randomly chosen during an actual application. Updraft positions should be held for 20 min of simulation time and then re-calculated to account for the duration of a typical updraft. Updraft duration can range from 5 to 30 min, indicating that this parameter should be varied during simulation testing of autonomous soaring algorithms.

VII. Future Work

The updraft model presented in this paper is useful for the development of autonomous soaring guidance and control but does not model all of the significant characteristics of naturally occurring updrafts. Naturally occurring updrafts have time dependant vertical velocities and radiuses. Additionally, naturally occurring updrafts drift and change shape when wind is present; and naturally occurring updrafts merge together to form larger and stronger updrafts as height increases. Downdrafts are also known to form along with updrafts during times of strong convection. Future updraft models, therefore, should include these effects as well as include convective scale parameters for locations and topographies other than the desert.

VIII. Concluding Remarks

This paper presented a model of convective updrafts using convective scale parameters calculated from ground and balloon measurements taken at Desert Rock, Nevada. Convective scale velocity and convective mixing layer thickness test cases were produced using statistical tools. Statistical representation did not include measurement data during times of zero convection, representing 25 percent of the total measurement set. A statistical representation of the convective mixing-layer thickness values corresponding to the set of convective scale velocities was produced by fitting the data to a Gamma probability density function. Convective scale parameters were then used to calculate mean updraft vertical velocity and radius using equations from Lenschow. The vertical velocity distribution within the updraft was calculated by fitting the data in Konovalov to a family of bell-shaped curves. The toroid structure of updrafts as height increases, described in Bradbury, was included in the vertical velocity distribution of this model. Updraft spacing was calculated from a relationship given in Lenschow; and environment sink was calculated using the conservation of mass. This paper also presented an example use of the equations within the paper using the MATLAB code provided in the appendices. Taken together, the equations given herein describe an updraft model that is suitable for the preliminary design and simulation of guidance and control for soaring uninhabited air vehicles.

Appendix A. MATLAB Code for Example Application

```
%This script will run a check case of the NASA DFRC updraft model.
%
%Michael J. Allen
%NASA Dryden Flight Research Center
%2005
%

%DEFINE UPDRAFT PARAMETERS
wstar=2.56; %selected w*, m/s
zi=1401; %selected zi, m
z=280; %test height, m
wgain=1; %multiplier on vertical velocity
rgain=1; %multiplier on radius

%DEFINE AREA
X=1000; %length of test area, m
Y=1000; %width of test area, m
A=X*Y; %test area, m^2

%CALCULATE OUTER RADIUS
zzi=z/zi;
r2=(.102*zz^(1/3))*(1-(.25*zz))*zi; %Equation 12 from updraft paper

%CALCULATE NUMBER OF UPDRAFTS IN GIVEN AREA
N=round(.6*Y*X/(zi*r2));

%SET PERTURBATION GAINS FOR EACH UPDRAFT
wgain(1:N)=1; %multiplier on vertical velocity
rgain(1:N)=1; %multiplier on radius

%PLACE UPDRAFTS IN A LINE (NORMALLY THIS IS DONE RANDOMLY)
for kn=1:N, %for each updraft
    xt(kn)=kn*X/(N+1);
    yt(kn)=kn*Y/(N+1);
end

%DEFINE GRID OF TEST LOCATIONS
xc=[0:10:X];
yc=[0:10:Y];
xx=xc'*ones(1,length(yc)); %create matrix of x values
yy=ones(length(xc),1)*yc; %create matrix of y values
zz=ones(size(xx)).*z; %create matrix of z values
for kx=1:length(xc),
    disp([num2str(kx) 'of ' num2str(length(xx))])
    for ky=1:length(yc),

        %CALL UPDRAFT FUNCTION
        w(kx,ky)=run_model2_3(xx(kx,ky),yy(kx,ky),zz(kx,ky),...
            xt,yt,wstar,wgain,rgain,zi,A,1);
    end
end

%PLOT UPDRAFT FIELD. THIS WILL CREATE FIGURE 11
figure; orient tall
    mesh(xx,yy,w)
```

```

xlabel('X position, m')
ylabel('Y position, m')
zlabel('w, m/s')
set(gca,'View',[-22 64])

```

```

%PLOT CROSS-SECTION OF 1ST UPDRAFT. THIS WILL CREATE FIGURE 12
figure; orient tall
h1=plot(yy(18,1:40),w(18,1:40),'k-'); grid
set(gca,'fontsize',12)
set(h1,'linewidth',2)
xlabel('y position, m')
ylabel('w, m/s')

```

Appendix B. MATLAB Code for Updraft Model

```

function [w,r2,wc] = ...
run_model2_3(x,y,z,xt,yt,wstar,wgain,rgain,zi,A,sflag)
%function [w,r2,wc] = run_model2_3(x,y,z,xt,yt,wstar,wgain,rgain,zi,A)
%
%Input:  x      = Aircraft x position (m)
%        y      = Aircraft y position (m)
%        z      = Aircraft height above ground (m)
%        xt     = Vector of updraft x positions (m)
%        yt     = Vector of updraft y positions (m)
%        wstar  = updraft strength scale factor, (m/s)
%        wgain  = Vector of perturbations from wstar (multiplier)
%        rgain  = Vector of updraft radius perturbations from average
%                (multiplier)
%        zi     = updraft height (m)
%        A      = Area of test space
%        sflag  = 0=no sink outside of thermals, 1=sink
%
%Output: w = updraft vertical velocity (m/s)
%        r2 = outer updraft radius, m
%        wc = updraft velocity at center of thermal, m/s
%
%
%Michael J. Allen, NASA DFRC, 2005

%DEFINE UPDRAFT SHAPE FACTORS
r1r2shape = [0.1400 0.2500 0.3600 0.4700 0.5800 0.6900 0.8000]';
Kshape = ...
    [1.5352    2.5826   -0.0113   -0.1950    0.0008;...
     1.5265    3.6054   -0.0176   -0.1265    0.0005;...
     1.4866    4.8356   -0.0320   -0.0818    0.0001;...
     1.2042    7.7904    0.0848   -0.0445    0.0001;...
     0.8816   13.9720    0.3404   -0.0216    0.0001;...
     0.7067   23.9940    0.5689   -0.0099    0.0002;...
     0.6189   42.7965    0.7157   -0.0033    0.0001];

%CALCULATE DISTANCE TO EACH UPDRAFT
N=length(xt);
for k=1:N,
    xdsq=(x-xt(k))^2;
    ydsq=(y-yt(k))^2;
    dist(k)=sqrt(xdsq+ydsq);
end

```



```

%CALCULATE AVERAGE UPDRAFT SIZE
zzi=z/zi;
rbar=(.102*zzi^(1/3))*(1-(.25*zzi))*zi;

%CALCULATE AVERAGE UPDRAFT STRENGTH
wtbar=(zzi^(1/3))*(1-1.1*zzi)*wstar;

%USE NEAREST UPDRAFT
upused=find(dist==min(dist));
if length(upused)>1; upused=upused(1); end

%CALCULATE INNER AND OUTER RADIUS OF ROTATED TRAPEZOID UPDRAFT
r2=rbar*rgain(upused); %multiply by random perturbation gain
if r2<10, %limit small updrafts to 20m diameter
    r2=10;
end
if r2<600,
    r1r2=.0011*r2+.14;
else,
    r1r2=.8;
end
r1=r1r2*r2;

%MULTIPLY AVERAGE UPDRAFT STRENGTH BY WGAIN FOR THIS UPDRAFT
wt=wtbar*wgain(upused); %add random perturbation

%CALCULATE STRENGTH AT CENTER OF ROTATED TRAPEZOID UPDRAFT
wc=(3*wt*((r2^3)-(r2^2)*r1)) / ((r2^3)-(r1^3));

%CALCULATE UPDRAFT VELOCITY
r=dist(upused);
rr2=r/r2; %r/r2
if z<zi, %if you are below the BL height
    if r1r2<.5*(r1r2shape(1)+r1r2shape(2)), %pick shape
        ka=Kshape(1,1);
        kb=Kshape(1,2);
        kc=Kshape(1,3);
        kd=Kshape(1,4);
    elseif r1r2<.5*(r1r2shape(2)+r1r2shape(3)),
        ka=Kshape(2,1);
        kb=Kshape(2,2);
        kc=Kshape(2,3);
        kd=Kshape(2,4);
    elseif r1r2<.5*(r1r2shape(3)+r1r2shape(4)),
        ka=Kshape(3,1);
        kb=Kshape(3,2);
        kc=Kshape(3,3);
        kd=Kshape(3,4);
    elseif r1r2<.5*(r1r2shape(4)+r1r2shape(5)),
        ka=Kshape(4,1);
        kb=Kshape(4,2);
        kc=Kshape(4,3);
        kd=Kshape(4,4);
    elseif r1r2<.5*(r1r2shape(5)+r1r2shape(6)),
        ka=Kshape(5,1);
        kb=Kshape(5,2);
        kc=Kshape(5,3);

```

```

        kd=Kshape(5,4);
    elseif rlr2<.5*(rlr2shape(6)+rlr2shape(7)),
        ka=Kshape(6,1);
        kb=Kshape(6,2);
        kc=Kshape(6,3);
        kd=Kshape(6,4);
    else,
        ka=Kshape(7,1);
        kb=Kshape(7,2);
        kc=Kshape(7,3);
        kd=Kshape(7,4);
    end

    in=rr2;

    %CALCULATE SMOOTH VERTICAL VELOCITY DISTRIBUTION
    ws = (1./(1+(ka.*abs(in+kc)).^kb))+kd*in;
    ws(find(ws<0))=0; %no neg updrafts
else,
    ws=0;
end %end if low enough

%CALCULATE DOWNDRAFT VELOCITY AT THE EDGE OF THE UPDRAFT
if dist(upused)>r1 & rr2<2,
    w1=(pi/6)*sin(pi*rr2); %downdraft, positive up
else,
    w1=0;
end
if zzi>.5 & zzi<=.9,
    swd=2.5*(zzi-.5); %scale factor for wd for zzi,
    %used again later

    wd=swd*w1;
    wd(find(wd>0))=0;
else,
    swd=0;
    wd=0;
end
w2=ws*wc+wd*wt; %scale updraft to actual
%velocity

%CALCULATE ENVIRONMENT SINK VELOCITY
At=N*pi*(rbar^2); %total area taken by updrafts
if At>A, error('Area of test space is too small'); return; end

if sflag,
    we=-(At*wtbar*(1-swd))/(A-At); %environment sink rate,
    %positive up (m/s)
    we(find(we>0))=0; %don't allow positive sink
else,
    we=0;
end

%STRETCH UPDRAFT TO BLEND WITH SINK AT EDGE
if dist(upused)>r1; %if you are outside the core
    w=w2*(1-we/wc)+we; %stretch
else,
    w=w2;
end

```

References

- ¹“Fédération Aéronautique Internationale (FAI) – Gliding World Records,” Fédération Aéronautique Internationale, URL: <http://records.fai.org/gliding/current.asp?id1=DO&id2=1> [cited 08 November 2005].
- ²Weimerskirch, Henri, Chastel, Olivier, Barbraud, Christophe, and Tostain, Olivier, “Frigatebirds Ride High on Thermals,” *Nature*, Vol. 421, January 23, 2003, pp. 333–334.
- ³Allen, Michael J. “Autonomous Soaring for Improved Endurance of a Small Uninhabited Air Vehicle,” AIAA-2005-1025, *43rd AIAA Aerospace Sciences Meeting*, Reno, NV, January 10–13, 2005.
- ⁴Metzger, Darryl E., and Hedrick, J. Karl, “Optimal Flight Paths for Soaring Flight,” AIAA 74-1001, *AIAA/MIT/SSA 2nd International Symposium on the Technology and Science of Low Speed and Motorless Flight*, Cambridge, Massachusetts, September 11–13, 1974.
- ⁵Cone, Clarence D., Jr., “The Design of Sailplanes for Optimum Thermal Soaring Performance,” NASA TN D-2052, 1964.
- ⁶Mostovoi, Gueorgui V., “Two-Dimensional Lagrangian Model of a Rising Thermal: Application for a Liquid Water Content Spatial Variability of a Warm Cumulus Cloud,” *Atmospheric Research* 43, 1997, pp. 233–252.
- ⁷Wharington, John, and Herszberg, Israel, “Control of a High Endurance Unmanned Air Vehicle,” ICAS-98-3,7,1, AIAA A98-31555, *21st ICAS Congress*, Melbourne, Australia, September 13–18, 1998.
- ⁸“The SURFRAD Network,” National Oceanic and Atmospheric Administration, URL: <http://www.srrb.noaa.gov/surfrad/index.html> [cited 27 September 2004].
- ⁹Stull, Roland B., *An Introduction to Boundary Layer Meteorology*, Kluwer Academic Publishers, Norwell, MA, ISBN 90-277-2769-4, 1994.
- ¹⁰Lenschow, D. H., and Stephens, P. L., “The Role of Thermals in the Convective Boundary Layer,” *Boundary-Layer Meteorology*, 19, 1980, pp. 509–532.
- ¹¹Bradbury, Tom, *Meteorology and Flight, A Pilot’s Guide to Weather*, 3rd Edition, A & C Black Ltd, London, Great Britain, ISBN 0-7136-4226-2, 2000.
- ¹²Wharington, John, and Herszberg, Israel, “Optimal Semi-Dynamic Soaring,” Royal Melbourne Institute of Technology, Melbourne, Australia, October 11, 1998.
- ¹³Reichmann, Helmut, *Cross Country Soaring*, Soaring Society of America, Inc., Hobbs, NM, ISBN 1-883813-01-8, 1993.
- ¹⁴Kononov, D. A., “On the Structure of Thermals,” 12th OSTIV Congress, Alpine, USA, 1970.